Inorganic Chemistry

Article

pubs.acs.org/IC

Photoisomerization and Proton-Coupled Electron Transfer (PCET) Promoted Water Oxidation by Mononuclear Cyclometalated Ruthenium Catalysts

Sumanta Kumar Padhi,[†] Ryoichi Fukuda,[‡] Masahiro Ehara,[‡] and Koji Tanaka*[,†,§]

[†]Department of Life and Coordination-Complex Molecular Science, Institute for Molecular Science, 5-1, Higashiyama, Myodaiji, Okazaki, Aichi 444-8787, Japan

[‡]Department of Theoretical and Computational Molecular Science, Institute for Molecular Science and Research Center for Computational Science, 38 Nishigo-Naka, Myodaiji, Okazaki 444-8585, Japan

[§]Institute for Integrated Cell-Material Sciences, Kyoto University, Funai Center #201, Kyoto University Katsura, Nishikyo-ku, Kyoto 615-8530, Japan

Supporting Information

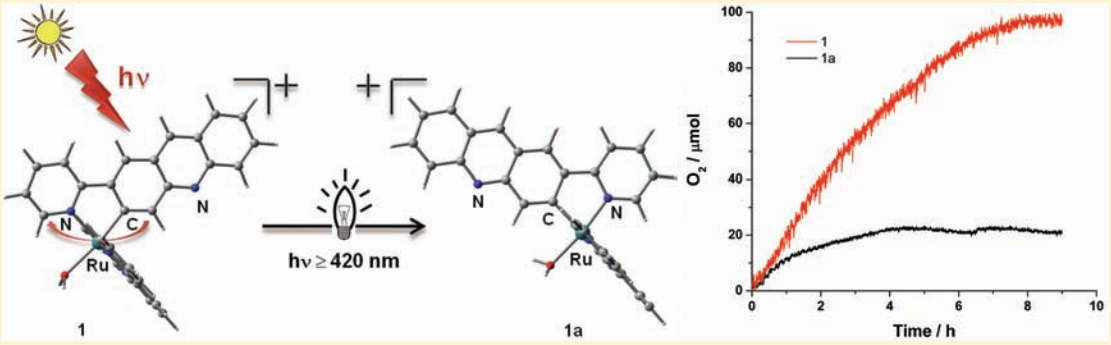

ABSTRACT: Photoisomeric transformations in ruthenium polypyridyl complexes have been rarely reported. Herein we report the geometrical transformation of cyclometalated *trans*-$[Ru(tpy)(PAD)(OH_2)]^+$ ($[\mathbf{1}]^+$) to the *cis*-$[Ru(tpy)(PAD)(OH_2)]^+$ ($[\mathbf{1a}]^+$) (tpy = 2,2′;6′,2″-terpyridine, PAD = 2-(pyrid-2′-yl)acridine) isomer upon irradiation of visible light ($\lambda \geq 420$ nm). Due to a proton-induced tautomeric equilibrium between the Ru−C bond and Ru═C coordination, the π^* energy levels of PADH are lower than those of tpy by 12.61 and 12.24 kcal mol^{-1}, respectively, in $[\mathbf{1}]^+$ and $[\mathbf{1a}]^+$. Isomers $[\mathbf{1}]^+$ and $[\mathbf{1a}]^+$ both act as catalytic oxygen-evolving complexes (OECs) chemically as well as electrochemically.

INTRODUCTION

Very few reports on the photoisomerization of polypyridyl ruthenium(II) aqua complexes are available: recently Yagi and co-workers reported the geometrical isomers of $[Ru(tpy)(pynap)OH_2]^{2+}$ (pynap = 2-(2-pyridyl)-1,8-naphthyridine)[1] and Meyer and co-workers studied the photoisomerization of *cis*-$[Ru(bpy)_2(OH_2)_2]^{2+}$ (bpy = 2,2′-bipyridine) to the trans form in water.[2]

Sustainable energy sources are the subject of much debate and are of ever-increasing interest at present. At present, to mitigate against a coming global disaster, science is searching for the sustainable energy resources which can convert solar energy to chemical energy and chemical energy to electrical energy.[3] Proton-coupled electron transfer (PCET) is a highly challenging area of research in aqueous media. Water can act as a proton acceptor as well as donor, and moreover the proton transfer in water remains in equilibrium.[4] The latest explanation of a competent water oxidation catalyst (WOC) also invokes the importance of the PCET process in the catalytic cycle.[5] Meyer et al. have revealed that proton-coupled electron transfer (PCET) reactions depend on the σ-donating and π-accepting abilities of the five ancillary ligands for ruthenium aqua complexes.[6] Oxygen evolution from water promoted by ruthenium complexes has recently been reviewed.[7] A number of mononuclear Ru(II) complexes that catalyze water oxidation have been identified and studied over the last few decades.[8] Monoaqua complexes, such as $[(bpy)_2(py)(H_2O)Ru^{II}]^{2+}$,[9] $[(tpy)(bpy)(H_2O)Ru^{II}]^{2+}$,[10] $[(tpy)(tmen)(H_2O)Ru^{II}]^{2+}$,[11] $[(tpy)(bpm)(H_2O)Ru^{II}]^{2+}$, and $[(tpy)(bpz)(H_2O)Ru^{II}]^{2+}$ (bpm = 2,2′-bipyrimidine, bpz = 2,2′-bipyrazine,[8c,d] tmen = *N*,*N*,*N*′,*N*′-tetramethylethylenediamine) exhibit two sequential one-electron−one-proton oxidations within the pH range of 1−7. The disproportionation of the Ru^{III} complex, which is thermodynamically favorable, sometimes leads to a two-electron oxidation process.[6,12]

Ce(IV) is used as an oxidant in most of the water oxidation reactions, where Ce(IV) acts as an oxidant in very strong acidic

Received: February 17, 2012
Published: April 23, 2012

   dx.doi.org/10.1021/ic3003542 | *Inorg. Chem.* 2012, 51, 5386−5392

aqueous solutions. The oxidation of water through electrochemical methods has several advantages, such as (i) regulation of the reaction conditions such as pH, (ii) applied potentials and solvents, and (iii) the ability to keep track of the durability of catalysts and efficiencies with the change of catalytic currents during the reactions. We have earlier demonstrated the utility of dinuclear ruthenium polypyridyl complexes with pendant bases, which act as water oxidation catalysts (WOCs) through electrochemical methods: e.g., $[Ru_2(OH)_2(3,6\text{-}t\text{-}Bu_2q)_2(btpyan)]^{2+}$, $[Ru_2(OH)_2(t\text{-}Bu_2sq)_2(btpyan)]^{0}$, $[Ru_2(OH)_2(Cl_2sq)_2(btpyan)]^{0}$, $[Ru_2(OH)_2(NO_2sq)_2(btpyan)]^{0}$, and $[Ru_2Cl_2(bpy)_2(btpyan)]$ (3,6-*t*-Bu_2q = 3,6-di-*tert*-butyl-1,2-benzoquinone, *t*-Bu_2sq = 3,6-di-*tert*-butyl-1,2-benzosemiquinone, Cl_2sq = 3,5-dichloro-1,2-benzosemiquinone, NO_2sq = 4-nitro-1,2-benzosemiquinone; bpy = 2,2′-bypiridyl, btpyan = 1,8-bis(2,2′:6′,2″-terpyrid-4′-yl)-anthracene).[13] To elucidate the role of pendant bases in the proton-coupled electron transfer (PCET) processes of ruthenium polypyridyl complexes, we have isolated the mononuclear cyclometalated isomers *trans*-$[Ru(tpy)(PAD)(OH_2)]^+$ ($[\mathbf{1}]^+$) and *cis*-$[Ru(tpy)(PAD)(OH_2)]^+$ ($[\mathbf{1a}]^+$) (tpy = 2,2′;6′,2″-terpyridine, PAD = 2-(pyrid-2′-yl)acridine). The isomers $[\mathbf{1}]^+$ and $[\mathbf{1a}]^+$ differ in the orientation of the asymmetric PAD ligand, as shown in Figure 1. The *trans*-

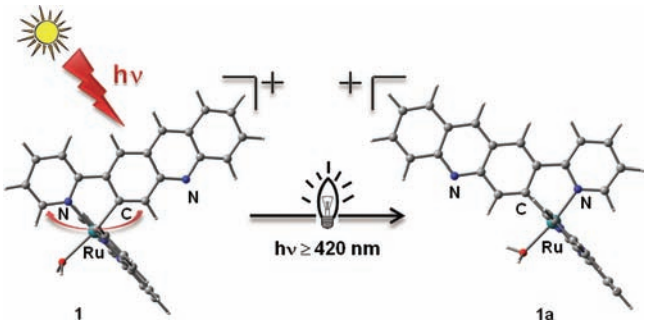

Figure 1. Photoisomerization from $[\mathbf{1}]^+$ to $[\mathbf{1a}]^+$ upon irradiation of visible light ($\lambda \geq 420$ nm).

$[Ru(tpy)(PAD)(OH_2)]^+$ ($[\mathbf{1}]^+$) and *cis*-$[Ru(tpy)(PAD)(OH_2)]^+$ ($[\mathbf{1a}]^+$) isomers are defined with respect to the coordinating carbon center relative to the aqua coordination. The geometrical difference and proton-induced tautomerism play a significant role in the properties of both the isomers. Here we present the redox and spectroscopic properties and report intriguing catalytic activity for the oxidation of H_2O in both isomers by chemical and electrochemical methods.

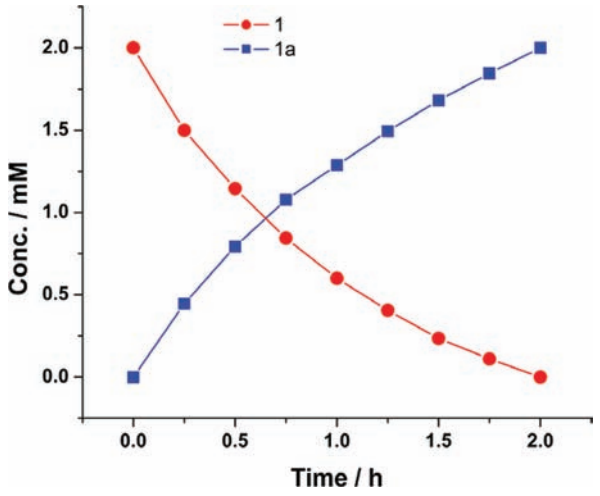

Figure 2. Change in concentration of both isomers during photoisomerization.

RESULTS AND DISCUSSION

Synthesis and Photoisomerization. The isomer $[\mathbf{1}]^+$ was synthesized by the ligand exchange reaction of $[Ru(PAD)(CH_3CN)_4](PF_6)$ with tpy and characterized by electrospray ionization (ESI) mass spectrometry and UV−vis and NMR spectroscopic analysis.[14] The photoisomerization process was conducted by a ^{1}H NMR based experiment. An NMR tube of 5 mm diameter fitted with an Young valve containing 2 mM of $[\mathbf{1}]^+$ in d_6-acetone was irradiated with visible light ($\lambda \geq 420$ nm) using a 100 W mercury lamp with a cutoff filter (0.5 M $NaNO_2$ solution) for 2 h. The ^{1}H NMR spectra of the reaction mixture were recorded at 25 min intervals. After 2 h it was noticed that transformation of the geometry from the trans to the cis isomer was complete. The kinetic profile (Figure 2) of the photoisomerization process was first order with respect to the concentration of $[\mathbf{1}]^+$, and the calculated rate constant $k = 23.90 \times 10^{-3}\ s^{-1}$ (at 293 K). For the other experimental studies $[\mathbf{1a}]^+$ was isolated in bulk amount utilizing a similar photoisomerization procedure. The internal quantum yield for the photoisomerization of $[\mathbf{1}]^+$ to $[\mathbf{1a}]^+$ was calculated to be 0.8%. The complex $[Ru(tpy)(PAD)(CH_3CN)]PF_6$ also shows

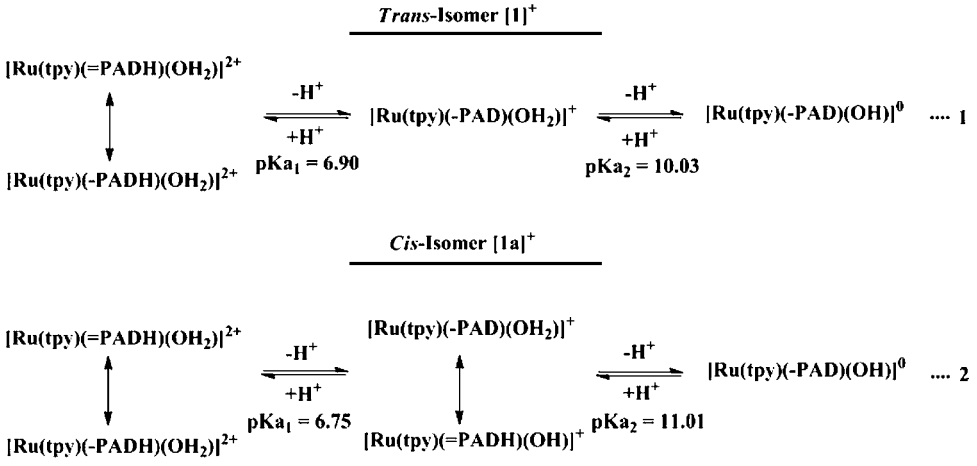

dx.doi.org/10.1021/ic3003542 | Inorg. Chem. 2012, 51, 5386−5392

Scheme 1. Tautomeric Equilibrium in $[\mathbf{1H}]^{2+}$

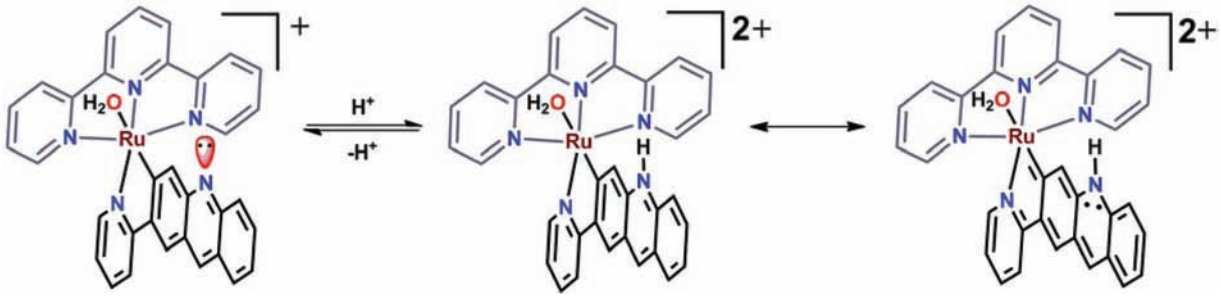

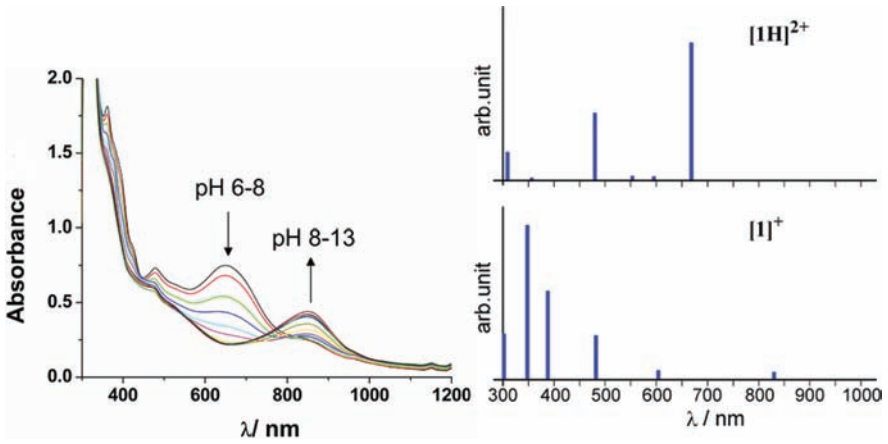

Figure 3. pH-dependent UV−vis spectra of $[\mathbf{1}]^+$ (left) and the oscillator strength (right).

photoisomerization with a slower rate ($k = 10.63 \times 10^{-2}$ s^{-1} (at 293 K)) as compared to the isomerization of $[\mathbf{1}]^+$.

Stability and Dynamic Equilibrium. Single crystals of these isomers could not be isolated after various attempts. Using the B3LYP DFT method with the 6-31G** basis set and LANL2DZ pseudopotential for Ru, the optimized structures of both configurations were determined for the singlet ground state (Tables S1 and S2, Supporting Information). Theoretically the isomerization energy was found to be 11.72 kcal mol^{-1} between $[\mathbf{1}]^+$ and $[\mathbf{1a}]^+$. The trans isomer $[\mathbf{1}]^+$ is comparatively more stable than the cis isomer $[\mathbf{1a}]^+$. The protonated form of the corresponding isomers at the noncoordinating nitrogen atom of the acridine moiety also exhibits similar behavior, where *trans*-$[Ru(tpy)(PADH)(OH_2)]^{2+}$ ($[\mathbf{1H}]^{2+}$) is more stable than *cis*-$[Ru(tpy)(PADH)(OH_2)]^{2+}$ ($[(\mathbf{1a})\mathbf{H}]^{2+}$) by 7.66 kcal mol^{-1}. The total energy difference between the optimized structures of $[\mathbf{1H}]^{2+}$ and $[\mathbf{1}]^+$ is 219.79 kcal mol^{-1}, whereas that between $[(\mathbf{1a})\mathbf{H}]^{2+}$ and $[\mathbf{1a}]^+$ is 223.85 kcal mol^{-1}. The higher stability is expected due to the Ru−C bond upon protonation, which exists in a tautomeric equilibrium with *r*NHC (remote N-heterocyclic carbene) Ru=C type coordination (Scheme 1).[14b] The π-accepting ability of the coordinated carbon center increases due to protonation at the pendant noncoordinating nitrogen atom of the acridine ring of both complexes, with a decrease of energy of the π^* orbital of PAD after protonation as compared to the nonprotonated form. The phenomenon of tautomeric equilibrium plays an important role during the electron and proton transfer processes.

Acid−Base Equilibria in the Complexes. Between pH 1 and 6, almost there is no change observed in the UV−vis spectra. The equilibrium in pH titration is noted in eqs 1 and 2, respectively, for $[\mathbf{1}]^+$ and $[\mathbf{1a}]^+$. In both cases, a significant decrease in band intensity occurs at 640−650 nm between pH 6 and 8. The deprotonation of $[Ru(tpy)(PAD)(OH_2)]^+$ occurs at higher pH, >8. Once the $[Ru(tpy)(PAD)(OH)]^0$ species was formed, there was no further spectral change with an increase in pH. This is due to the fully occupied t_{2g} orbitals of Ru^{II}, which cannot accept the π-character electrons.[5b,15] Therefore, proton dissociation from the $Ru^{II}(OH)$ complexes hardly takes place.[13d]

The UV−vis spectra of both the configurations were theoretically calculated using the SAC-CI method with LANL2DZ basis. The results for $[\mathbf{1}]^+$ are displayed in Figure S15 and Tables S3 and S4 (Supporting Information). The lowest singlet excited state of $[\mathbf{1}]^+$ was calculated at 830 nm. This state corresponds to the observed peak at 850 nm (ε = 4400 M^{-1} cm^{-1}) at higher pH. This state has the transition from HOMO to LUMO and HOMO-1 to LUMO. The HOMO and HOMO-1 of $[\mathbf{1}]^+$ have the character of a π orbital of PAD and also a d orbital of Ru, and the LUMO of $[\mathbf{1}]^+$ is a π^* orbital of tpy; therefore, this state has a CT character from PAD and Ru to tpy. The lowest singlet excited state of $[\mathbf{1H}]^{2+}$ was calculated at 668 nm. This state corresponds to the observed peak at 650 nm (ε = 7500 M^{-1} cm^{-1}) at lower pH. This state has the transition from HOMO to LUMO. The HOMO of $[\mathbf{1H}]^{2+}$ has the character of a π orbital of PADH and also a d orbital of Ru, and the LUMO is a π^* orbital of PADH; therefore, this state has a $\pi \rightarrow \pi^*$ transition character and also a CT character from Ru to PADH (Figure 3). The LUMO energy level of tpy is lower than that of PAD by 20.77 kcal mol^{-1} in $[\mathbf{1}]^+$. However, upon protonation the reverse trend is observed, where the π^* energy level of PADH is lower than that of tpy by 12.61 kcal mol^{-1}. This clearly reveals that the

dx.doi.org/10.1021/ic3003542 | Inorg. Chem. 2012, 51, 5386−5392

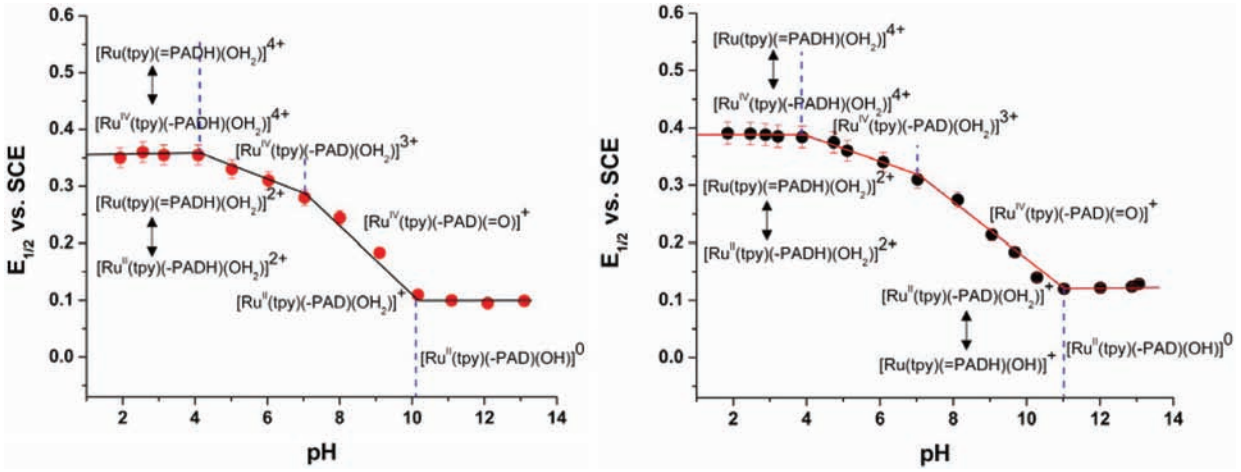

Figure 4. Pourbaix plots of $[\mathbf{1}]^+$ (left) and $[\mathbf{1a}]^+$ (right).

protonation alternates the character of the lowest electronic transition.

The results of the SAC-CI calculation for the cis isomers $[\mathbf{1a}]^+$ and $[(\mathbf{1a})\mathbf{H}]^{2+}$ were similar to those for the trans isomers. The results for $[\mathbf{1a}]^+$ are given in Figure S16 and Tables S5 and S6 (Supporting Information). The observed band at 640 nm (ε = 4000 M^{-1} cm^{-1}) is assigned to the lowest excitation of $[(\mathbf{1a})\mathbf{H}]^{2+}$ calculated at 668 nm. The observed peak at 850 nm (ε = 7200 M^{-1} cm^{-1}) at lower pH may be assigned to the lowest excitation of $[\mathbf{1a}]^+$ calculated at 914 nm; the calculated very low intensity can be attributed to the small basis sets. The cis isomer $[\mathbf{1a}]^+$ may exist even at lower pH, and *cis*-$[Ru(tpy)(PAD)(OH)]^+$ may be produced at higher pH. After the initial dissociation *cis*-$[Ru(tpy)(PAD)(OH_2)]^+$ may be in equilibrium with *cis*-$[Ru(tpy)(PADH)(OH)]^+$. The DFT calculation shows that *cis*-$[Ru(tpy)(PAD)(OH_2)]^+$ is more stable compared to *cis*-$[Ru(tpy)(PADH)(OH)]^+$ by 4.45 kcal mol^{-1}, but in the trans isomer *trans*-$[Ru(tpy)(PAD)(OH_2)]^+$ is more stable compared to *trans*-$[Ru(tpy)(PADH)(OH)]^+$ by 13.66 kcal mol^{-1} . Therefore, a small change in the UV−vis spectra of isomer $[\mathbf{1a}]^+$ isobserved at pH >7.

Aqueous Electrochemistry. The initial oxidation process in both the isomers $[\mathbf{1}]^+$ (within the pH range 1.95−4.0) is a pH independent $2e^-$ oxidation process of $[Ru(tpy)(=PADH)(OH_2)]^{2+}/[Ru(tpy)(=PADH)(OH_2)]^{4+}$. Between pH 4 and 11, the CV of $[\mathbf{1}]^+$ displays the two oxidation events $[Ru(tpy)(=PADH)(OH_2)]^{2+}/[Ru(tpy)(-PAD)(OH_2)]^{3+}$ (pH range 4−7) and $[Ru^{II}(tpy)(-PAD)(OH_2)]^+/[Ru^{IV}(tpy)(-PAD)(=O)]^+$ (pH range 7−11) with slopes of −30 mV per pH unit and −60 mV per pH unit, indicating that they are $2e^-/1H^+$ and $2e^-/2H^+$ processes, respectively (Figure 4 (left)). Consumption of 2 F/mol of electrons in the exhaustive electrolysis of the 0.5 mM complex in buffer solution at various pHs (2−10) was clarified by bulk electrolysis. At higher pH both these isomers exhibit pH-independent oxidation potentials. The nature of the oxidation process in $[\mathbf{1a}]^+$ is almost similar to that of $[\mathbf{1}]^+$; the only difference is in pK_a (Figure 4 (right)) values. The pK_{a1} and pK_{a2} values in the case of $[\mathbf{1}]^+$ are observed at 6.90 and 10.03, respectively, whereas in isomer $[\mathbf{1a}]^+$, they are at 6.75 and 11.01. The pK_a values resembles those determined from the pH titration of UV−vis spectra. The potential of the second anodic wave observed at higher potentials was difficult to determine, since it appeared as a broad shoulder in the strong catalytic current.

For both isomers $[\mathbf{1}]^+$ and $[\mathbf{1a}]^+$, the first oxidation process was examined using the chemical oxidant $(NH_4)_2[Ce(NO_3)_6]$ (CAN) in 0.1 M HNO_3. In case of isomer $[\mathbf{1}]^+$, upon addition of up to 2 equiv of CAN, the peaks in the UV/vis absorption spectrum at 650 nm decreased in intensity with isosbestic points at 455 and 390 nm (Figure S17, Supporting Information). In isomer $[\mathbf{1a}]^+$ the absorption intensity at 530 nm increases along with a decrease at 850 nm upon addition of 2 equiv of CAN (Figure S18, Supporting Information), confirming a concerted path for the $2e^-$ oxidation process in each isomer. In both cases it is also chemically reversible with the addition of 2 equiv of $(NH_4)_2Fe(SO_4)_2$, as the reduction of the newly formed solution (after addition of 2 equiv of Ce(IV)) takes place, resulting in the starting isomers (Figure S19 and S20, Supporting Information).

Catalytic Activity for Water Oxidation. Isomers $[\mathbf{1}]^+$ and $[\mathbf{1a}]^+$ show catalytic activity for water oxidation with an excess of the sacrificial oxidant CAN (Figure 5). For the calculation of

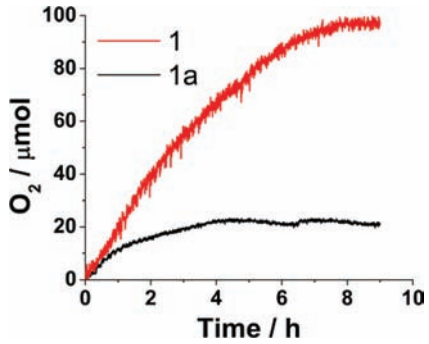

Figure 5. Dioxygen evolution with the addition of 80 nM complex into a 16 mM CAN solution in 0.1 M HNO_3.

turnover number (TON), 10 nM of complex catalyst was used with 16 mM CAN in 0.1 M HNO_3. The oxygen evolved was detected with an Ocean Optics O_2 probe up to a constant concentration of O_2. The catalytic activity of the cis isomer $[\mathbf{1a}]^+$ is lower than that of the trans isomer $[\mathbf{1}]^+$ with respective TON values of 1200 and 3500. It was found that the catalytic activities depend on the concentrations of both Ce(IV) and catalyst. The initial rate with respect to the concentration of either Ce(IV) or the complex catalyst is first order in nature (Figures S22−S25, Supporting Information) in both isomers.

dx.doi.org/10.1021/ic3003542 | Inorg. Chem. 2012, 51, 5386−5392

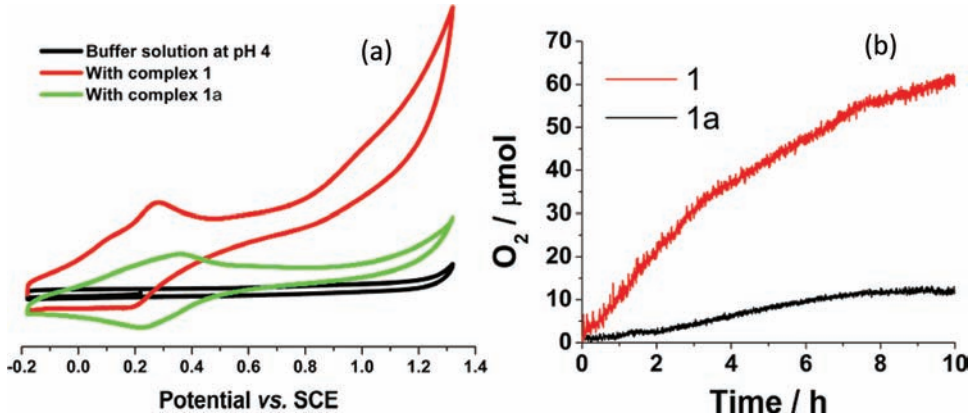

Figure 6. (a) Catalytic dioxygen evolution by the complexes at pH 4. (b) Dioxygen evolution by the isomers by electrochemical methods at pH 4.0 and potential 1.40 V vs SCE.

In comparison to the catalytic abilities of similar reported kinds of mononuclear ruthenium aqua complexes $[\mathbf{1}]^+$ has a remarkable ability for dioxygen evolution from water.[16]

The cyclic voltammogram (CV) of $[\mathbf{1}]^+$ in an aqueous solution at pH 1.95 exhibited a redox couple at 0.31 V and that of $[\mathbf{1a}]^+$ at 0.33 V (vs SCE), assigned to Ru^{II}/Ru^{III} (Figure S26, Supporting Information). The subsequent strong anodic currents (Figure 6a) at potentials more positive than +1.4 V vs (SCE) are associated with water oxidation (Figure 6b), also clearly observed in the cyclic voltammogram. The controlled-potential electrolysis of $[\mathbf{1}]^+$ and $[\mathbf{1a}]^+$ at +1.40 V vs SCE catalytically evolved dioxygen in water at pH 4.0 (buffered with H_3PO_4/KOH). The oxygen evolved in the working compartment of the H-type cell was detected with an Ocean Optics O_2 probe until a constant concentration of O_2. The catalytic behavior is very low as compared to the chemical catalysis. The catalytic activity of the trans isomer $[\mathbf{1}]^+$ is relatively higher than that of the cis isomer $[\mathbf{1a}]^+$ with respective TON values of 30 and 6. The higher catalytic ability of the trans isomer is expected, due to the lower pK_{a2} value compared to that of the cis isomer as well as due to the contribution by trans effect of the σ-donating as well as π-accepting ability of carbon coordination. It leads to destabilization of the Ru−OH_2 bond and induces a partial positive polar character at the oxygen atom of the aqua ligand, which facilitates the attack by another water molecule to evolve dioxygen.

CONCLUSION

Upon visible light ($\lambda \geq 420$ nm) irradiation, photoisomerization takes place from cyclometalated *trans*-$[Ru(tpy)(PAD)(OH_2)]^+$ ($[\mathbf{1}]^+$) to the isomer *cis*-$[Ru(tpy)(PAD)(OH_2)]^+$ ($[\mathbf{1a}]^+$). Upon protonation the Ru−C bond exists in a tautomeric equilibrium with Ru═C coordination, which plays a significant role in proton-coupled electron transfer (PCET). This is in agreement with the theoretically predicted geometries and the experimental UV−vis results. In both cases, the LUMO energy levels of PAD drastically decrease from the π^* energy levels of the tpy ligand upon protonation. These isomers show catalytic water oxidation ability in chemical and electrochemical methods. The isomer $[\mathbf{1}]^+$ is a better catalyst than $[\mathbf{1a}]^+$. The catalytic activity by chemical oxidation methods also shows that $[\mathbf{1}]^+$ comes within that of the reported better mononuclear ruthenium based catalytic oxygen-evolving complexes (OECs) such as d-$[Ru(tpy)(pynap)(OH_2)](PF_6)_2$ (d = distal) (TON = 3200), d-$[Ru(tpy)(pynap)(Cl)](PF_6)$ (TON = 2700).[16] To the best of our knowledge, this is the first example of a mononuclear cyclometalated ruthenium complex which behaves as a water oxidation catalyst (WOC) in electrochemical methods. The mechanistic approach for water oxidation in both methods is underway and will be published later in detail. The higher catalytic activity of trans isomer in comparison to that of the cis isomer is expected, due to the lower pK_{a2} value in comparison to that of the cis isomer and the contribution by trans effect of the carbon coordination.

EXPERIMENTAL SECTION

Instrumentation and Materials. All the manipulations were carried out using standard Schlenk techniques under a nitrogen atmosphere. The solvents acetonitrile, acetone, and ethanol were dried, degassed, and stored under a nitrogen atmosphere prior to use. The ligand 2-pyridylacridine (PAD) and $[Ru(PAD)(CH_3CN)_4]PF_6$ were synthesized by following our reported procedure.[14b] NMR spectra were recorded on a JEOL JNM-A500 spectrometer (500 MHz for ^1H) at room temperature. High-resolution ESI mass spectra were recorded on a Waters Micromass LCT. The UV−vis−near-IR spectra were recorded on a Shimadzu UVPC-3100 PC UV−vis−near-IR scanning spectrophotometer. The photoisomerization was carried out by visible light ($\lambda \geq 420$ nm) using a 100 W mercury lamp with a cutoff filter (0.5 M $NaNO_2$ solution).

Both cyclic voltammetry and controlled-potential electrolysis were carried out under an argon atmosphere. Cyclic voltammetry was carried out using an ALS/Chi Model 660A electrochemical analyzer under an argon atmosphere at 25 °C at a scan rate of 50 mV. Aqueous electrochemistry experiments were performed with 0.5 mM solutions of the complex due to limited solubility. Between pH 1.5 and 13.5, solutions containing 0.1 M H_3PO_4 were used after adjusting the pH with KOH. The experimental conditions were as follows: working electrode, ITO; counter electrode, Pt wire; reference electrode, Ag/$AgNO_3$; experiments conducted in a one-compartment cell.

Bulk controlled-potential electrolysis was carried out in deionized water buffered with H_3PO_4/NaOH (pH 4.0) at room temperature. The electrolysis cell used in the study consisted of three compartments: one for the indium−tin oxide working electrode (15 mm × 30 mm), the second for a platinum counter electrode (15 mm × 30 mm) that was separated from the working electrode cell by a cation exchange membrane (Nafion 117, Sigma-Aldrich Co.), and the third for the $Ag/AgNO_3$ reference electrode. The oxygen sensor was attached to the working electrode cell. One of the complexes {*trans*-$[Ru(tpy)(PAD)(OH_2)]PF_6$ ($[\mathbf{1}](PF_6)$) and *cis*-$[Ru(tpy)(PAD)(OH_2)]PF_6$ ($[\mathbf{1a}](PF_6)$) (1.5 mg, 2.0 μmol)} was added to the aqueous phase in the working electrode. Both solutions were purged by argon through in the working and counter electrode cells for 30 min to remove O_2 before electrolysis. Electrolysis of the solution was carried out with a Hokuto Denko HA-501 potentiostat and an HF201

dx.doi.org/10.1021/ic3003542 | *Inorg. Chem.* 2012, 51, 5386−5392

coulomb meter. The oxygen concentration was recorded by an oxygen sensor at +1.100 V vs $Ag/AgNO_3$. After 2.0 F/mol of electricity was consumed, the electrolysis was stopped. The concentration of oxygen in the solution was monitored until it became constant.

Oxygen measurements were performed using a calibrated O_2 probe (Ocean Optics Foxy sport probe). A single-point reset was performed prior to catalysis run. The reaction vessel was a 150 mL two-necked round-bottom flask with two side arms equipped with Teflon plugs to allow gas flow and oxidant injection, and the third neck was modified to accommodate the O_2 probe. The gastight vessel was equipped with a stir bar at room temperature. In a typical experiment to determine turnover number, the oxidant $Ce(NH_4)_2(NO_3)_6$ (16 mM, 20 mL of 0.1 M HNO_3) was injected into the vessel and degassed by purging argon and the vessel was charged with a solution of the ruthenium complex (concentration 10 nM) (the resulting pH of the solution is ~1.8). The vessel was sealed, and the O_2 generated over the course of 12 h was monitored.

Synthesis. *Synthesis and Isolation of [Ru(tpy)(PAD)(CH$_3$CN)]PF$_6$.* To a solution of (0.400 g, 0.60 mmol) of $[Ru(PAD)(CH_3CN)_4]PF_6$ in 50 mL of ethanol was added with 0.140 g (0.6 mmol) of tpy (=2,2′;6′,2″-terpyridine). The reaction mixture was refluxed at 80 °C for 12 h. The crude product was evaporated to dryness and recrystallized from acetonitrile solution to give $[Ru(tpy)(PAD)(CH_3CN)]PF_6$ (0.355 g, 0.46 mmol; yield 76%). It was characterized by ESI-MS, UV−visible, and NMR spectroscopic measurements. HRMS (ESI): calcd for $C_{35}H_{25}N_6Ru$ $[\mathbf{1}]^+$ m/z 631.12, found 631.46; calcd for $[\mathbf{1} - CH_3CN]^+$ m/z 590.09, found 590.38. Anal. Calcd for $C_{35}H_{25}F_6N_6PRu$: C, 54.20; H, 3.25; N, 10.83. Found C, 54.34; H, 3.29; N, 10.81. The ^{1}H NMR (500 MHz, CD_3CN): δ, ppm (J, Hz) 1.96 (3H, s), 6.53 (1H, s), 7.25 (2H, t, 6.40), 7.57 (1H, t, 7.6), 7.69 (1H, t, 7.00), 7.74 (3H, d, 6.1), 7.87 (H, t, 7.63), 7.96 (1H, t, 7.65), 8.14 (2H, t, 8.55), 8.19 (1H, t, 7.9), 8.34 (2H, d, 7.90), 8.44−8.48 (4H, m), 9.30 (1H, s), 9.50 (1H, d, 4.90).

Synthesis and Isolation of trans-[Ru(tpy)(PAD)(OH$_2$)]PF$_6$ ([1](PF$_6$)). A solution of 0.200 g (0.26 mmol) of $[Ru(tpy)(PAD)(CH_3CN)]PF_6$ in 50 mL of acetone/H_2O (8/2 v/v) was refluxed at 80 °C for 7 h. The reaction mixture was evaporated to dryness followed by a minimum addition of acetone and precipitated with the addition of water. The dark pink precipitate was centifuged and washed several times with water to give pure *trans*-$[Ru(tpy)(PAD)(OH_2)]PF_6$ ($[\mathbf{1}](PF_6)$; 0.175 g, 0.23 mmol; yield 89%). It was characterized by ESI-MS, UV−visible, and NMR spectroscopic measurements. HRMS (ESI): calcd for $[\mathbf{1} - OH_2]^+$ m/z 590.09, found 590.38; calcd for $[\mathbf{1} - H]^{2+}$ m/z 303.54, found 303.53. Anal. Calcd for $C_{33}H_{24}F_6N_5OPRu$: C, 52.66; H, 3.21; N, 9.31. Found: C, 52.74; H, 3.23; N, 9.34. ^{1}H NMR (500 MHz, CD_3CN): δ, ppm (J, Hz) 6.49 (1H, s), 7.22 (1H, t, 6.42), 7.27 (2H, t, 6.1), 7.36 (1H, t, 7.32), 7.52 (1H, d, 5.5), 7.67−7.76 (3H, m), 7.81−7.85 (2H, m), 7.91−7.98 (2H, m), 8.06−8.14 (2H, m), 8.41−8.48 (2H, m), 8.54 (1H, d, 7.9), 8.67 (1H, d, 7.95), 8.93 (2H, d, 7.95), 8.96 (s, OH_2), 9.49 (1H, d, 4.85).

Synthesis and Isolation of cis-[Ru(tpy)(PAD)(OH$_2$)]PF$_6$ ([1a](PF$_6$)). Visible light ($\lambda \geq 420$ nm) was irradiated into a solution of 0.100 g (0.13 mmol) of *trans*-$[Ru(tpy)(PAD)(OH_2)]PF_6$ in 25 mL of acetone over 24 h using a 100 W mercury lamp with a cutoff filter (0.5 M $NaNO_2$ solution). The reaction mixture was evaporated to dryness, 1 mL of acetone was added, and the product precipitated with the addition of water. The light pink precipitate was centifuged and washed several times with water to give pure *cis*-$[Ru(tpy)(PAD)(OH_2)]PF_6$ ($[\mathbf{1}](PF_6)$; 85 mg, 0.11 mmol; yield 86%). It was characterized by ESI-MS, UV−visible, and NMR spectroscopic measurements. HRMS (ESI): calcd for $[\mathbf{1} - OH_2]^+$ m/z 590.09, found 590.38; calcd for $[\mathbf{1} - H]^{2+}$ m/z 303.52, found 303.53. Anal. Calcd for $C_{33}H_{24}F_6N_5OPRu$: C, 52.66; H, 3.21; N, 9.31. Found C, 52.71; H, 3.25; N, 9.29. ^{1}H NMR (500 MHz, CD_3CN): δ, ppm (J, Hz) 7.33 (1H, t, 7.32), 7.35 (s, OH_2), 7.41 (1H, t, 6.1), 7.45 (1H, t, 6.7), 7.62 (1H, t, 7.6), 7.71 (1H, d, 4.9), 7.86 (1H, t, 8.25), 7.94−8.00 (2H, m), 8.08 (1H, t, 8.55), 8.17−8.21 (3H, m), 8.27 (1H, d, 9.15), 8.57 (1H, td, 7.90 and 7.95), 8.66 (1H, d, 11), 8.69−8.71 (2H, m), 8.77 (1H, d, 10), 8.81 (1H, d, 7.9), 8.89 (1H, d, 2.45), 9.09 (1H, d, 7.9), 9.14 (1H, s).

■ ASSOCIATED CONTENT

Supporting Information

Figures and tables giving synthesis details, characterization data, experimental details, data for DFT calculations. This material is available free of charge via the Internet at http://pubs.acs.org.

■ AUTHOR INFORMATION

Corresponding Author

*E-mail: ktanaka@ims.ac.jp and koji.tanaka@icems.kyoto-u.ac.jp.

Notes

The authors declare no competing financial interest.

■ ACKNOWLEDGMENTS

This work was supported by a Grant-in-Aid for Specially Promoted Research (Grant 20002005) from the Ministry of Education, Culture, Sports, Science, and Technology of Japan.

■ REFERENCES

(1) Yamazaki, H.; Hakamata, T.; Komi, M.; Yagi, M. *J. Am. Chem. Soc.* **2011**, *133*, 8846−8849.

(2) Durham, B.; Wilson, S. R.; Hodgson, D. J.; Meyer, T. J. *J. Am. Chem. Soc.* **1980**, *102*, 600−607.

(3) (a) Nocera, D. G. *ChemSusChem* **2009**, *2*, 387−390. (b) Eisenberg, R.; Nocera, D. G. *Inorg. Chem.* **2005**, *44*, 6799−6801. (c) Lewis, N. S.; Nocera, D. G. *Proc. Natl. Acad. Sci. U.S.A.* **2006**, *103*, 15729−15735. (d) Armaroli, N.; Balzani, V. *Angew. Chem., Int. Ed.* **2006**, *46*, 52−66. (e) Lewis, N. S. *Science* **2007**, *315*, 798−801. (f) Tanaka, K. *Chem. Rec.* **2009**, *9*, 169−186.

(4) Costentin, C. *Chem. Rev.* **2008**, *108*, 2145−2179.

(5) (a) Eisenberg, R.; Gray, H. B. *Inorg. Chem.* **2008**, *47*, 1697−1699. (b) Huynh, M. H. V.; Meyer, T. J. *Chem. Rev.* **2007**, *107*, 5004−5064. (c) Chang, C. J.; Chang, M. C. Y.; Damrauer, N. H.; Nocera, D. G. *Biochim. Biophys. Acta* **2004**, *1655*, 13−28. (d) Kanan, M. W.; Nocera, D. G. *Science* **2008**, *321*, 1072−1075. (e) Surendranath, Y.; Dinca, M.; Nocera, D. G. *J. Am. Chem. Soc.* **2009**, *131*, 2615−2620.

(6) Dovletoglou, A.; Adeyemi, S. A.; Meyer, T. J. *Inorg. Chem.* **1996**, *35*, 4120−4127.

(7) (a) Romain, S.; Vigara, L.; Llobet, A. *Acc. Chem. Res.* **2009**, *42*, 1944−1953. (b) Concepcion, J. J.; Jurss, J. W.; Brennaman, M. K.; Hoertz, P. G.; Patrocinio, A. O. T.; Iha, N. Y. M.; Templeton, J. L.; Meyer, T. J. *Acc. Chem. Res.* **2009**, *42*, 1954−1965.

(8) (a) Concepcion, J. J.; Jurss, J. W.; Templeton, J. L.; Meyer, T. J. *Proc. Natl. Acad. Sci. U.S.A.* **2008**, *105*, 17632−17635. (b) Tseng, H.-W.; Zong, R.; Muckerman, J. T.; Thummel, R. *Inorg. Chem.* **2008**, *47*, 11763−11773. (c) Concepcion, J. J.; Jurss, J. W.; Templeton, J. L.; Meyer, T. J. *J. Am. Chem. Soc.* **2008**, *130*, 16462−6463. (d) Chen, Z.; Concepcion, J. J.; Jurss, J. W.; Meyer, T. J. *J. Am. Chem. Soc.* **2009**, *131*, 15580−15581. (e) Concepcion, J. J.; Tsai, M.-K.; Muckerman, J. T.; Meyer, T. J. *J. Am. Chem. Soc.* **2010**, *132*, 1545−1557. (f) Concepcion, J. J.; Jurss, J. W.; Norris, M. R.; Chen, Z. F.; Templeton, J. L.; Meyer, T. J. *Inorg. Chem.* **2010**, *49*, 1277−1279. (g) Wasylenko, D. J.; Ganesamoorthy, C.; Koivisto, B. D.; Henderson, M. A.; Berlinguette, C. P. *Inorg. Chem.* **2010**, *49*, 2202−2209.

(9) Moyer, B. A.; Meyer, T. J. *J. Am. Chem. Soc.* **1978**, *100*, 3601−3603.

(10) Takeuchi, K. J.; Thompson, M. S.; Pipes, T. J.; Meyer, T. J. *Inorg. Chem.* **1984**, *23*, 1845−1851.

(11) Ho, C.; Che, C.; Lay, T. *J. Chem. Soc., Dalton Trans.* **1990**, 967−970.

(12) Masllorens, E.; Rodriguez, M.; Romero, I.; Roglans, A.; Parella, T.; Benet-Buchholz, J.; Poyatos, M.; Llobet, A. *J. Am. Chem. Soc.* **2006**, *128*, 5306−5307.

(13) (a) Muckerman, J. T.; Polyansky, D. E.; Wada, T.; Tanaka, K.; Fujita, E. *Inorg. Chem.* **2008**, *47*, 1787−1802. (b) Wada, T.; Tsuge, K.; Tanaka, K. *Inorg. Chem.* **2001**, *40*, 329−337. (c) Wada, T.; Tsuge, K.; Tanaka, K. *Angew. Chem., Int. Ed.* **2000**, *39*, 1479−1482. (d) Wada, T.; Muckerman, J. T.; Fujita, E.; Tanaka, K. *Dalton Trans.* **2011**, *40*, 2225−2233.
(14) (a) Padhi, S. K.; Tanaka, K. *Inorg. Chem.* **2011**, *50* (21), 10718−10723. (b) Padhi, S. K.; Kobayashi, K.; Masuno, S.; Tanaka, K. *Inorg. Chem.* **2011**, *50* (12), 5321−5323.
(15) Meyer, T. J.; Huynh, M. H. V. *Inorg. Chem.* **2003**, *42*, 8140−8160.
(16) Boyer, J. L.; Polyansky, D. E.; Szalda, D. J.; Zong, R.; Thummel, R. P.; Fujita, E. *Angew. Chem.* **2011**, *123*, 12808−12812.